

## A metamodeling approach for studying ignition target robustness in a highly dimensional parameter space

Jean Giorla,<sup>1</sup> Annie Masson,<sup>1</sup> Françoise Poggi,<sup>1</sup> Robert Quach,<sup>1</sup> Patricia Seytor,<sup>1</sup> and Josselin Garnier<sup>2</sup>

<sup>1</sup>Commissariat à l'Énergie Atomique, DAM, DIF, F-91297 Arpajon, France

<sup>2</sup>Laboratoire de Probabilités et Modèles Aléatoires and Laboratoire Jacques-Louis Lions, UFR Mathématiques, Case 7012, Université Paris VII, 2 Place Jussieu, 75251 Paris Cedex 5, France

(Received 22 October 2008; accepted 9 February 2009; published online 31 March 2009)

Inertial confinement fusion targets must be carefully designed to ignite their central hot spots and burn. Changes in the optimal implosion could reduce the fusion energy or even prevent ignition. Since there are unavoidable uncertainties due to technological defects and not perfect reproducibility from shot to shot, the fusion energy will remain uncertain. The degree with which a target can tolerate larger specifications than specified, and the probability with which a particular yield is exceeded, are possible measures of the robustness of that design. This robustness must be assessed in a very high-dimensional parameter space whose variables include every characteristics of the given target and of the associated laser pulse shape, using high-fidelity simulations. Therefore, these studies would remain computationally very intensive. In this paper we propose an approach which consist first of constructing an accurate metamodel of the yield on the whole parameter space with a reasonable data set of simulations. Then the robustness is very quickly assessed for any set of specifications with this surrogate. The yield is approximated by a neural network, and an iterative method adds new points in the data set by means of D-optimal experimental designs. The robustness study of the baseline Laser Mégajoule target against one-dimensional defects illustrates this approach. A set of 2000 simulations is sufficient to metamodel the fusion energy on a large 22-dimensional parameter space around the nominal point. Furthermore, a metamodel of the robustness margin against all specifications has been obtained, providing guidance for target fabrication research and development. © 2009 American Institute of Physics.

[DOI: [10.1063/1.3091920](https://doi.org/10.1063/1.3091920)]

### I. INTRODUCTION

The objective of the French inertial confinement fusion (ICF) program is to burn cryogenic deuterium-tritium (DT) capsules indirectly driven with the Laser Mégajoule (LMJ) facility.<sup>1</sup> At the end of the implosion, fusion initiates in a central hot spot, and a thermonuclear burn front propagates into the main dense fuel.<sup>2</sup> Several features are important in the implosion process, and target design is a trade-off between different risks of nonignition, such as shell break-up, kinetic energy ignition margin, laser-plasma instabilities, etc. As there are several design parameters, we have developed an analytical model<sup>3</sup> to explore the whole parameter space and find potential targets in the laser energy-power field constrained by the LMJ capabilities. Afterward, one-dimensional (1D) and two-dimensional (2D) simulations are performed to precisely design these potential targets by optimizing the laser pulse shape, the beam pointing and the hohlraum size.

Finally, robustness studies must be conducted to estimate the yield sensitivity to all the technological errors and imperfections and to set the specifications. For a given optimized target, the yield  $Y$  is a function of all these errors  $\mathbf{X} = (X_1, \dots, X_N)$ . As these flaws will be different from shot to shot, the implosion process and the fusion energy delivered at a particular experiment remains uncertain. Then we regard  $\mathbf{X}$  as a random input vector, which induces a random yield  $Y(\mathbf{X})$  and more generally random outputs as peak velocity  $v$ ,

fuel entropy  $S$ , hot spot deformation, and so on. Therefore, the robustness of that target could be defined by different metrics which quantify these uncertainties. A possible metric is the probability  $P(Y > y_0)$  with which a particular yield  $y_0$  will be exceeded. Another robustness measure is the specification margin defined by the multiplier  $M$  of all the parameter specifications  $\{\xi_i, i=1, \dots, N\}$  which induces a probability  $P_M(Y > y_0) = 0.5$ .  $\xi_i$  could be either a standard deviation, a tolerance, or a surface roughness. As the yield is a strongly nonlinear function, with cliffs in most directions, and as the random parameters could be very numerous, these robustness measures are extremely difficult to assess.

The random input factors are generally split into two broad categories for numerical reasons: variabilities that are 1D in character, keeping the implosion spherical, and variabilities that deform the capsule, which are fundamentally three-dimensional (3D) but whose effects are often estimated with 2D-simulations. Since final deformation is easier to model than 3D-yield, a first method to assess the robustness margin versus 3D effects is to use a metric based on the distance between the mean root mean square (rms) deformation and the deformation threshold.<sup>4</sup> As low mode deformations remain linear, it is even possible to obtain the 3D-rms probability distribution function for a broad range of parameters such as 180 laser defects (60 power errors, 120 mis-pointing), five targets positioning errors, and 12 hohlraum

fabrication defects.<sup>5</sup> However, the final deformation is not enough in order to quantify the robustness as 1D quantities such as peak velocity and fuel entropy could be modified as well.

In order to overcome this challenging difficulty, Haan *et al.*<sup>6</sup> recently proposed an approach that consists first to model the four final variables  $v$ ,  $S$ , hot spot rms at ignition time, and fuel/ablator rms at peak velocity versus all uncertainties, and then to define an ignition margin as a function of these four quantities, based on scaling laws whose coefficients was extracted from a huge data set of at least 10 000 1D-simulations,<sup>7</sup> 2000 2D-simulations,<sup>8</sup> and a few 3D-simulations.<sup>9</sup>

In this paper, we propose an alternative approach which consists of directly constructing an accurate metamodel of the yield on the uncertainty parameter space with a reasonable data set of simulations, without assuming any *a priori* formulation of the yield response surface. Then the robustness will be very quickly evaluated for any set of specifications with this surrogate that is without any additional high resolution simulation.

The construction of a yield metamodel in a high-dimensional parameter space has remained a challenge until the recent progress in the field of experimental designs with nonlinear functions.<sup>10,11</sup> In order to demonstrate the feasibility of this approach, we have studied the 1D-robustness of a FCI target in a parameter space of dimension 22. The yield is approximated by a neural network, and an iterative method adds new points in the data set by means of D-optimal experimental designs. Finally, only a few thousands simulations are necessary to obtain an accurate metamodel.

This paper is organized as follows. The following section describes the LMJ ignition design chosen as an illustration of the metamodeling approach and the 1D parameters of the robustness study. Section III explains and applies the methodology for metamodeling the fusion energy in a very high-dimensional space. Section IV then summarizes the results obtained with this metamodel, principally in terms of yield probabilities and specification margins. The impact of variables such as central gas fill density, DT aging, and preheating is presented. Section V addresses another advantage of this approach, which consists of quickly evaluating the robustness sensitivity to the standard deviations  $\sigma_i$  of all random parameters. The following formula of the total 1D-margin  $M$ :  $M^{-2} = \sum_i k_i \sigma_i^2$  is proved in the Appendix for a fairly general form of the yield versus parameters and compared to a metamodel  $M^{-2} = f(\sigma_i)$  obtained by an experimental design. Section VI concludes.

## II. BASE LINE AND 1D PARAMETERS

The basis of this study is the A1040 LMJ capsule design shown in Fig. 1. This capsule encased in a gold cylindrical hohlraum is the baseline design for the full LMJ using 240 beams.<sup>3</sup> The A1040 capsule encased in a “rugby-shaped” hohlraum is also a candidate for the first ignition attempts that will be undertaken with 160 beams before the total facility completion.<sup>12,13</sup> The spherical capsule is composed of a 100  $\mu\text{m}$  thick cryogenic deuterium-tritium shell with an ex-

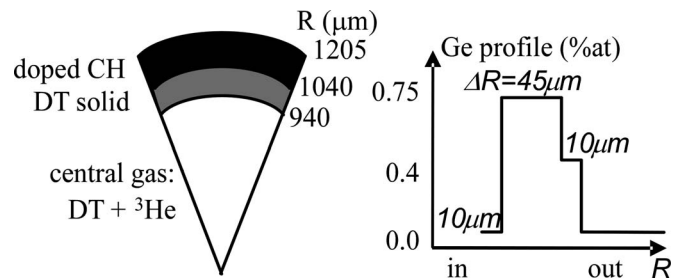


FIG. 1. The A1040 capsule is composed of a cryogenic DT layer surrounded by a CH ablator doped with germanium. The dopant profile in the three inner CH layers is drawn on the right plot.

ternal radius of 1040  $\mu\text{m}$ , covered by a plastic (CH) ablator nonuniformly doped with germanium. The ablator includes two pure CH layers surrounding two doped layers to reduce the growth of short wavelength hydrodynamic instabilities.<sup>14</sup> The central gas consists of DT gas in equilibrium with the solid DT phase and of  $^3\text{He}$  gas created by  $\beta$ -decay. Finally, the capsule is driven by a carefully tuned radiation pulse reaching a peak temperature of 300 eV and leading to a sequence of four shocks in the DT ice. The thickness of the outer CH layer is adjusted so that it remains a nonablated mass of 40–50  $\mu\text{g}$  at peak velocity. As the fraction of oxygen in the ablator is greater than the previously used one, the opacities and equations of state are slightly different, leading to an optimized outer radius of 1205  $\mu\text{m}$  instead of 1215  $\mu\text{m}$  as obtained before.<sup>14</sup> The nominal 1D-yield  $Y_0$  is about 32 MJ.

Even in 1D, the number of parameters that could potentially change the fusion energy is huge. In order to demonstrate the feasibility of the metamodeling approach, we have limited this first study to only the 22 following parameters: nine drive temperature shape parameters as defined in Fig. 2, nine ablator variables (density, outer radius, total thickness, three inner layer thicknesses, two germanium proportions and the oxygen proportion), three DT parameters (ice thickness, DT and  $^3\text{He}$  partial densities in the gas), and one DT preheating level. The DT partial density is correlated with the cryogenic temperature compatible with a good DT ice roughness, and the amount of  $^3\text{He}$  depends on the filling process. The DT preheat consists of a constant power-weight ratio deposited in the whole fuel during the main pulse. It is a rough estimation of the real effects of hot electrons and hard x-rays that are not taken into account in these capsule-only simulations.

The three last parameters play a particular role: The DT and  $^3\text{He}$  gas densities depend on the cryogenic process that is not set today and the preheating level is an unknown variable. It is therefore important to estimate the robustness against these design or unknown parameters. In order to achieve the specification margin defined in Sec. I, the metamodel  $Y = F(\mathbf{x})$  was constructed on a hypercube around the nominal point  $\mathbf{x}_0 = (x_{1,0}, \dots, x_{22,0})$ , which covers at least  $\pm 5$  nominal standard deviation  $\sigma_{i,0}$  for each stochastic parameter, the whole possible space for the two gas densities, and a level of preheating which ranges from 0 to a value larger

temperature

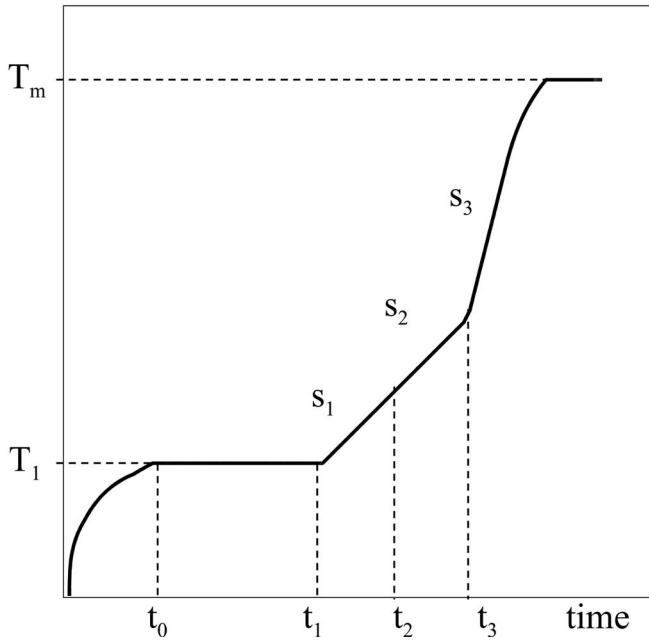


FIG. 2. The radiation pulse is parameterized with an analytical law depending on four times  $t_0$  to  $t_3$ , three slopes  $s_1$  to  $s_3$  and two temperatures  $T_1$  and  $T_m$ .

than the ignition threshold. Table I sums up the 22 parameters taken into account with their nominal values, the ranges used for metamodeling the yield and the nominal standard deviations used for evaluating the robustness.

### III. METAMODELING THE FUSION ENERGY

The metamodeling approach consists of replacing a complex computer code by a mathematical approximation called a response surface, a surrogate or a metamodel, which links the code output  $Y$  to the input vector  $\mathbf{x}$  for a specific class of problems.<sup>10</sup> Our goal is to obtain this approximation from a reasonable set of simulations judiciously chosen. The main difficulty of metamodeling the fusion energy of an ICF capsule is due to the very complicated shape of the response surface  $Y(\mathbf{x})$  with cliffs followed by a plateau ( $Y \approx 0$ ) in almost all directions. Among the several possible metamodels we have tested, the best one is a particular form of a neural network<sup>15</sup> with a single layer of  $K$  hidden neurons based on tangent hyperbolic functions,

$$Y(\mathbf{x}) = \tanh \left[ \omega_{00} + \sum_{k=1, K} \omega_{0k} \tanh \left( \sum_{i=1, 22} \omega_{ik} x_i \right) \right].$$

Here, the input parameters  $\mathbf{x} = (x_1, \dots, x_{22})$  defined in Sec. II and the yield  $Y$  are scaled to the unit hypercube. The neural network parameters  $\omega$  are estimated from two databases: a training set to find possible parameters and a validation set to select the best ones. The accuracy of the surrogate is then quantified by the root mean square error (RMSE) between the metamodel and the simulation outputs on a third database named test set. As the neural network is non linear against its parameters  $\omega$ , the choice of the training set is not obvious. The classical procedure is to construct a first experimental design where the inputs are uniformly sampled, and then to incrementally add new points. However, a uniform sampling fails to sample points with nonzero yield which are located near the origin because the volume of the unit sphere is

TABLE I. List of the 1D-parameters taken into account. Variables  $x_1$  to  $x_9$  define the temperature pulse shape;  $x_{10}$  to  $x_{18}$  are relative to the ablator fabrication;  $x_{19}$  to  $x_{21}$  concern the DT ice conformation; and  $x_{22}$  is the unknown deposited energy in the fuel.

Parameters		Nominal values $x_{i,0}$	Ranges	Nominal standard deviations $\sigma_{i,0}$
$x_1$	Plateau temperature $T_1$	$0.9 \times 10^6$ K	$\pm 80 \times 10^3$ K	$11 \times 10^3$ K
$x_2$	Peak temperature $T_m$	$3.5 \times 10^6$ K	$\pm 280 \times 10^3$ K	$44 \times 10^3$ K
$x_3$	First slope $s_1$		$\pm 0.06$ MK/ns	0.006 MK/ns
$x_4$	Second slope $s_2$		$\pm 0.3$ MK/ns	0.022 MK/ns
$x_5$	Third slope $s_3$		$\pm 0.3$ MK/ns	0.039 MK/ns
$x_{6-9}$	Times $t_0, t_1, t_2,$ and $t_3$		$\pm 400$ ps	50 ps
$x_{10}$	Outer ablator radius	1205 $\mu\text{m}$	$\pm 40$ $\mu\text{m}$	4 $\mu\text{m}$
$x_{11}$	Total ablator thickness	165 $\mu\text{m}$	$\pm 40$ $\mu\text{m}$	6 $\mu\text{m}$
$x_{12}$	Inner CH layer thickness	10 $\mu\text{m}$	$\pm 7$ $\mu\text{m}$	1.2 $\mu\text{m}$
$x_{13}$	CHGe <sub>0.75</sub> layer thickness	45 $\mu\text{m}$	$\pm 30$ $\mu\text{m}$	2.7 $\mu\text{m}$
$x_{14}$	CHGe <sub>0.40</sub> layer thickness	10 $\mu\text{m}$	$\pm 7$ $\mu\text{m}$	1.2 $\mu\text{m}$
$x_{15}$	Ge in CHGe <sub>0.40</sub>	0.40 at. %	$\pm 0.4$ at. %	0.04 at. %
$x_{16}$	Ge in CHGe <sub>0.75</sub>	0.75 at. %	$\pm 0.75$ at. %	0.08 at. %
$x_{17}$	Oxygen in CH	4 at. %	$\pm 2$ at. %	0.8 at. %
$x_{18}$	Ablator density	1.07 g/cm <sup>3</sup>	$\pm 0.1$ g/cm <sup>3</sup>	0.012 g/cm <sup>3</sup>
$x_{19}$	DT ice thickness	100 $\mu\text{m}$	$\pm 30$ $\mu\text{m}$	2 $\mu\text{m}$
$x_{20}$	DT gas density	0.3 mg/cm <sup>3</sup>	(0.18; 0.5 mg/cm <sup>3</sup> )	0.01 mg/cm <sup>3</sup>
$x_{21}$	<sup>3</sup> He gas density	0	(0; 0.2 mg/cm <sup>3</sup> )	...
$x_{22}$	DT preheating	0	(0; $5.10^{12}$ erg/g)	...

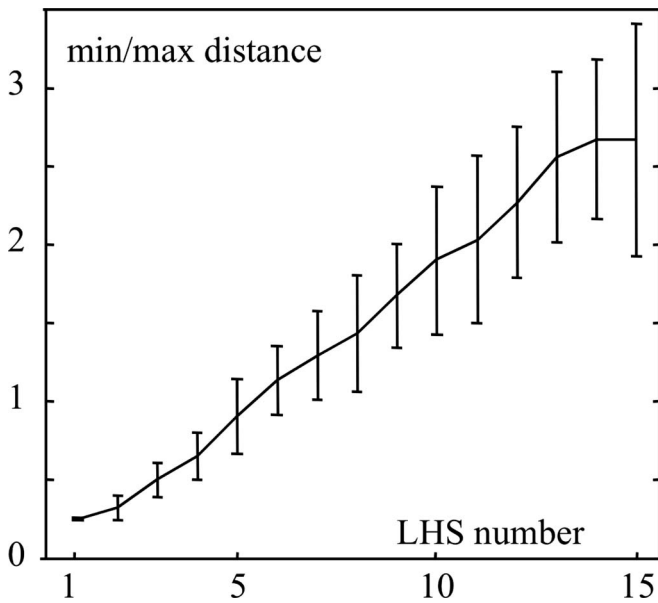


FIG. 3. Minimum/maximum intervals for the first 510 points sampled in 15 onion LHS.

$1 \times 710^{-9}$  smaller than the volume of the hypercube  $[-1, +1]^{22}$ . To overcome this other challenging difficulty, we have constructed a first set of 510 points with 15 Latin hypercube samplings<sup>17</sup> (LHSs) fitted into each other on  $[-a_i, +a_i]^{22}$ , where  $a_i = 15/i$ . Each LHS, which consists of 34 points sampled on 34 levels, was chosen in order to maximize the minimal distance between two points as shown in Fig. 3. The validation and test sets consist of 15 and seven onions LHS with 150 and 120 points, respectively, built in the same way.

A first network was created from these first simulation runs, and a set of new points was added to the training set using the D-optimality criterion, as proposed in Ref. 11. The principle of the method is based on the Fisher information matrix  $M_F$  which is locally defined as  $M_F = J^T J$ , where  $J$  is the Jacobian matrix  $J = [\partial Y(x_k) / \partial \omega_{ij}]$  of the nonlinear neural network model. From a large set of candidate points, the Fedorov exchange algorithm<sup>18</sup> is applied to select a subset that maximizes the determinant of  $M_F$ . As we can see in Fig. 4, the D-optimal criterion adds points in the ignition cliff where the yield variations are the largest. As the new training set is larger, we can increase the number of hidden units in the neural network and the accuracy of the yield surrogate. This procedure was repeated twice, and the final surface response  $Y(\mathbf{x})$  was defined as the median of the 50 best neural networks in the sense of the smallest training and validation mean square errors. We have obtained a RMSE of 2.1 MJ that is small enough for the robustness study, as we will see on the next section. On the whole, we have run 2078 simulations and the final neural networks are composed of 18 hidden units and 433 parameters.

Since this first study, the method was applied to another ICF capsule and the accuracy was increased by adding new points to the data set with a criterion of maximal discrepancy between the 50 best networks. The authors have obtained a RMSE of 0.6 MJ (4.5% of the nominal yield) with 3322 simulations.

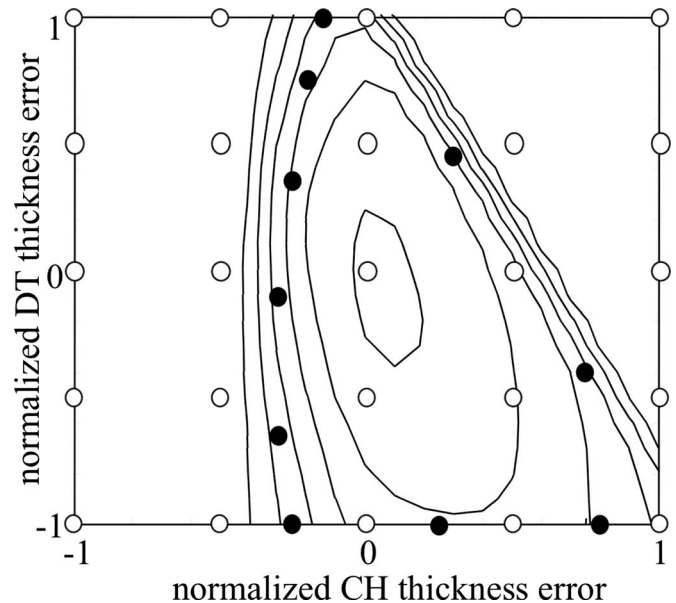


FIG. 4. Example in two dimensions. The lines are the yield contours, the white circles correspond to the first sampling and the black circles to the points added with the D-optimal criterion. They are located where the yield gradient is maximal.

#### IV. APPLICATION TO YIELD PROBABILITY AND ROBUSTNESS MARGIN

As part of the 22 input parameters will be different from shot to shot, we regard them as random variables. The statistical distribution of the yield is then evaluated by a Monte Carlo method where the metamodel is used in place of the 1D-code.

##### A. Independent sources of uncertainties

We do not take into account a stochastic error for the parameters  $x_{21}$  and  $x_{22}$  ( $^3\text{He}$  density and preheating level). The random deviations on the inputs  $x_1$  and  $x_2$  (plateau and peak temperatures) are correlated and come from five independent errors  $S_1$  to  $S_5$ : the two measurement errors, the hohlraum fabrication defect, the incident laser power stability, and the beam scattering reproducibility due to laser-plasma instability (LPI). The random deviations on  $x_3$  and  $x_{20}$  are independent sources of errors. On the whole, there are 23 independent random variables that lead to dispersions on the input parameters  $x_1$  to  $x_{20}$ . The nominal standard deviations are listed in Tables I and II. They are based on CEA

TABLE II. List of five independent sources of errors that modify the two temperature input parameters  $T_1$  and  $T_m$ . The errors on  $T_1$  and  $T_m$  due to  $S_3$  or  $S_4$  are fully correlated.

( $10^3$ K)	Sources of errors	$\sigma_{T_1}$	$\sigma_{T_m}$
$S_1$	Experimental error on $T_1$	9.0	...
$S_2$	Experimental error on $T_m$	...	35.0
$S_3$	hohlraum fabrication defect	1.4	5.6
$S_4$	Laser power stability	5.4	21.0
$S_5$	LPI reproducibility	...	1.6

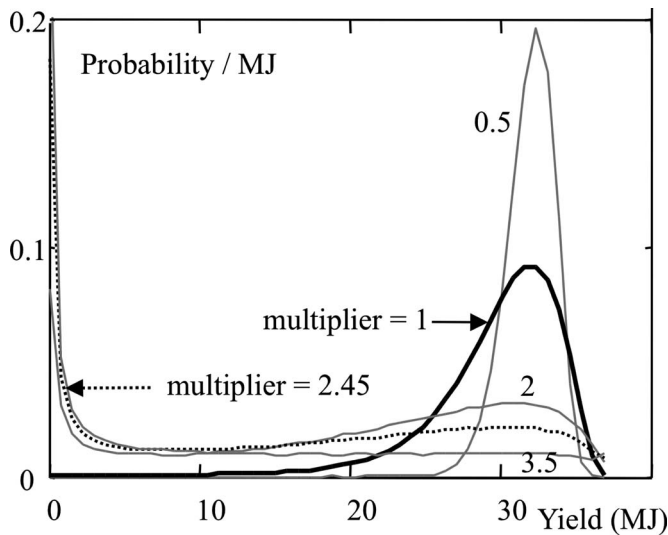


FIG. 5. Probability distribution functions of the 1D-yield for various multipliers of the nominal standard deviations.

fabrication capabilities achieved at the beginning of the study, laser specifications and pulse shape errors induced by inaccuracy on temperature and shock timing diagnostics.<sup>5</sup>

### B. Quantification of the yield uncertainty

The statistical distribution of the yield is evaluated by a Monte Carlo method where the 23 sources of errors are sampling according to their probability distribution functions (PDFs). The use of a metamodel instead of a computer code allows us to rapidly evaluate the yield PDF, even with 10 000 samplings needed for good accuracy. We have chosen Gaussian input PDFs in this first study, but there is no difficulty in using other distributions such as top-hat or truncated-Gaussian functions. The huge advantage of the metamodeling approach is that we do not have to run a new set of expensive simulations if we change these input PDFs. For example, it is very easy to estimate the yield distribution for different multipliers  $m$  of all the nominal standard deviations, as shown in Fig. 5: The PDF shape is localized near the nominal yield  $Y_0=32$  MJ for small dispersions on the input errors ( $m=0.5$ ) and is nearly flat for large errors ( $m=3.5$ ), except a peak at  $Y=0$  that corresponds to the proportion of nonignited targets. The corresponding cumulative probabilities are plotted in Fig. 6.

The probability to exceed a given fusion energy is a possible metric of the robustness of an ICF target. Another measure is the degree with which the target can tolerate larger specifications than specified. This specification margin was first defined by Haan *et al.*<sup>4</sup> as the multiplier  $M$  of all standard deviations leading to a probability of 0.5 to exceed half the nominal yield. The influence of the probability and yield thresholds which define the margin are plotted in Fig. 7. The variations are quasilinear for a threshold  $y_0$  between 10% and 90% of the nominal yield. The specification margin could also be evaluated for a subset of the input errors, as shown in Fig. 8, which is very useful in order to balance the specifications. This figure would have been impossible to

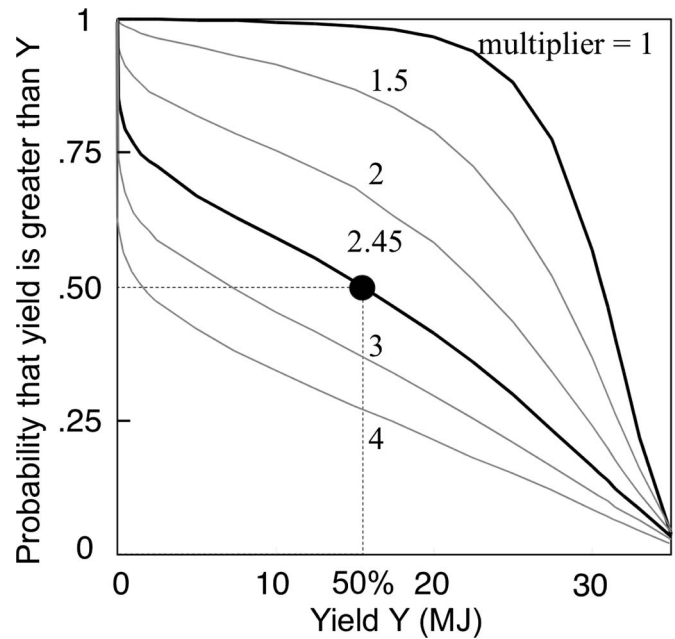


FIG. 6. Inverse cumulative probability of the yield for different multipliers of the nominal standard deviations.

obtain without a yield surrogate as each point corresponds to a Monte Carlo evaluation. The metamodeling error ( $\sigma_Y = 2.1$  MJ) leads to a margin error  $\sigma_M$  given by the following equation in first approximation:

$$\sigma_M \approx |\partial M / \partial Y| \sigma_Y \approx 0.13.$$

We mention that the stopping criterion for the iterative construction of the metamodel described in Sec. III is the estimation of  $\sigma_Y$ .

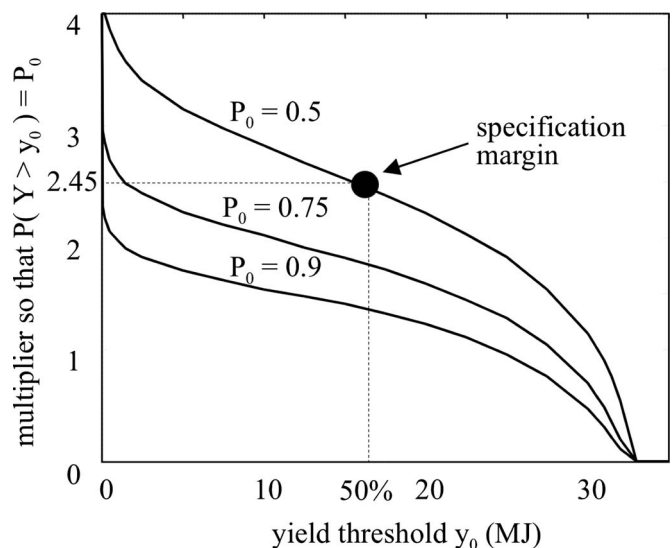


FIG. 7. Standard deviation multiplier that gives a probability of  $P_0$  to exceed a given yield  $y_0$ . The specification margin is the multiplier for  $P_0=0.5$  and  $y_0=Y_0/2$ .

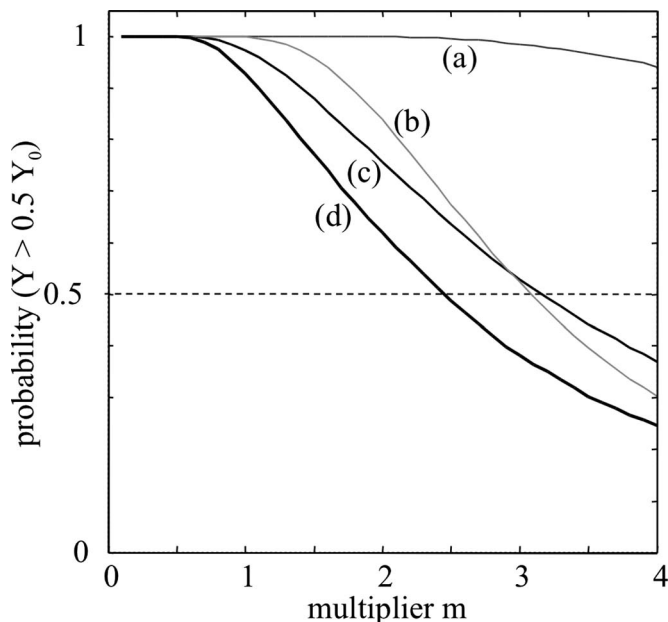


FIG. 8. Probability to exceed half the nominal yield as a function of the standard deviation multiplier for different subsets of input errors: (a) laser variations only; (b) experimental tuning uncertainties; (c) capsule errors; (d) all errors together.

### C. Sensitivity toward design or unknown parameters

The above results are relative to the robustness against the dispersions of parameters around the nominal design point  $\mathbf{x}_0$  defined by a DT gas density of  $0.3 \text{ mg/cm}^3$ , without  $^3\text{He}$  in the central gas and no preheating. These two central gas densities depend on the cryogenic process that is not definitively set today and the exact preheating level is unknown. It is therefore important to estimate the margin sensitivity to these three parameters  $x_{20}$  to  $x_{22}$ . We can notice that the capsule acceleration phase is not modified if we only change these inputs. In particular, the time intervals between the consecutive shock times in the solid DT remain the same, and the nominal pulse shape is still the optimal one in that sense. Thus, we have estimated the effect of these three parameters on the margin without modifying the other specified values  $x_1$  to  $x_{19}$ .

Once again, the metamodel allows us to estimate these sensitivities very quickly. The effect of central gas densities is illustrated in Fig. 9: In first approximation, the 1D-margin depends on a linear combination of the two densities as the isolines are mostly parallel. This is true for all preheating levels, and we have found that a function of the form given by Eq. (1) is a good approximation of the 1D-margin as we can see in Fig. 10,

$$F(u, h) = \log[a + bu + ch + du^2 + euh], \quad (1)$$

with  $u = \exp(\rho_{^3\text{He}} + 0.8\rho_{\text{DT}})$  and  $h$  the preheating.

For the specific case  $h=0$ ,  $F(u, h) \approx \log[89 - 92u + 24u^2]$  with the densities in  $\text{mg/cm}^3$ . The RMSE between this formulation and the 1D-margin is 0.05 on the full design of 605 points ( $11 \times 11 \times 5$ ) plotted in Fig. 10. It follows that an increase in  $^3\text{He}$  density of  $0.1 \text{ mg/cm}^3$  (12 days of  $\beta$ -decays)

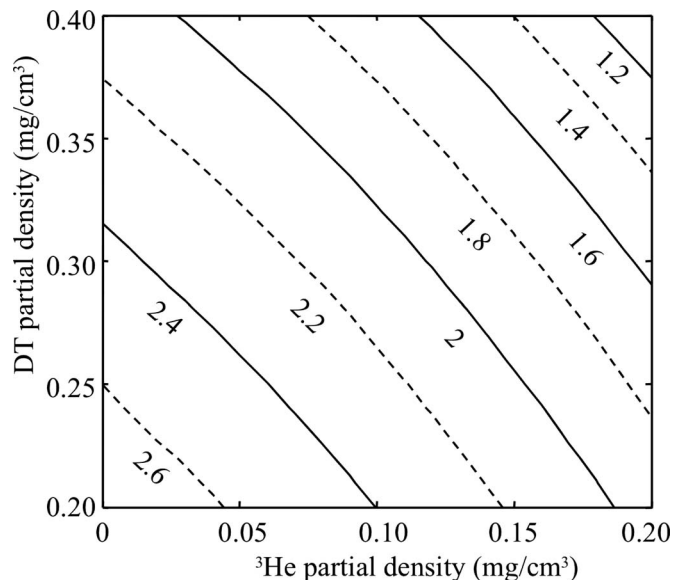


FIG. 9. Contour plot of the margin with respect to the central gas densities, without DT preheating. A  $^3\text{He}$  density of  $0.1 \text{ mg/cm}^3$  corresponds to 12 days of  $\beta$ -decay.

is equivalent to an increase in central gas DT of  $0.08 \text{ mg/cm}^3$  (that is a rise of about  $0.4 \text{ K}$  in the cryogenic temperature).

### V. MODELING THE MARGIN TOWARD THE PARAMETER STANDARD DEVIATIONS

The specification margin  $M$  is defined such that  $P_M(Y > y_0) = P_0$ , where  $P_M$  is the probability distribution obtained when all input random errors ( $X_i, i=1, \dots, N$ ) have their standard deviations  $\sigma_i$  multiplied by  $M$ . We can suppose that the random vector  $\mathbf{X}$  has zero mean. Haan *et al.*<sup>4</sup> proposed to estimate  $M$  by the following formula:

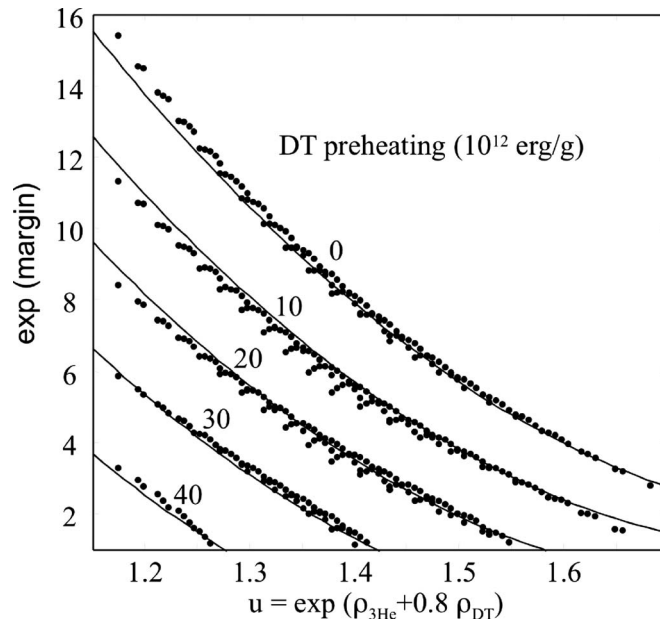


FIG. 10.  $\exp(\text{margin})$  for  $0 < \rho_{^3\text{He}} < 0.2 \text{ mg/cm}^3$ ,  $0.2 < \rho_{\text{DT}} < 0.4 \text{ mg/cm}^3$ , and a preheating of  $0/10/20/30/40 \text{ erg/g}$  (dots). The lines correspond to the approximation given by Eq. (1).

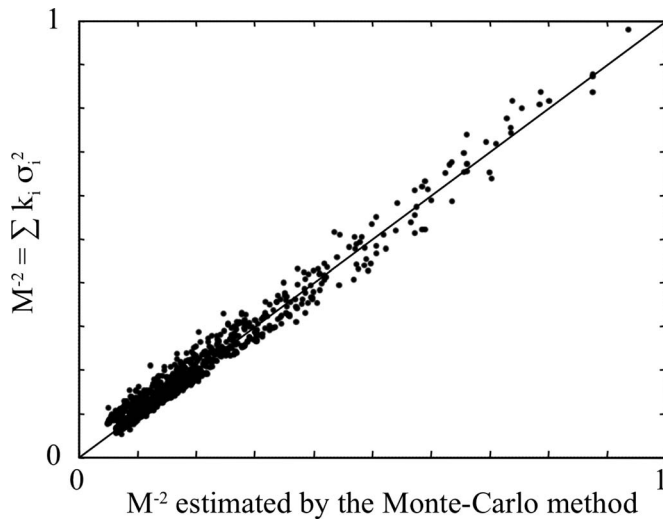


FIG. 11. Scatter plot for the prediction of the total margin given by Eq. (2).

$$M^{-2} \approx \sum_{i=1}^N M_i^{-2}.$$

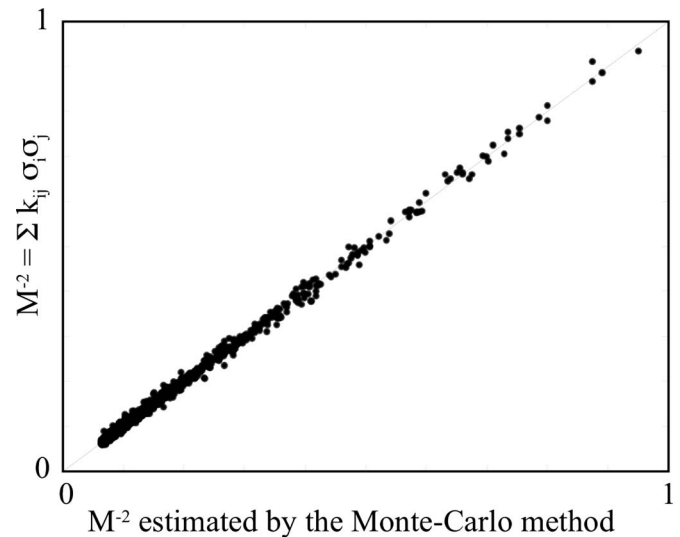
Here the partial margin  $M_i$  is the highest multiple of the nominal requirement  $\sigma_i$  that returns at least a yield  $y_0$ , in simulations in which  $X_i$  is the only error.  $M_i$  is inversely proportional to  $\sigma_i$  and it follows that the margin could be approximated by a quadrature sum of the standard deviations,

$$M^{-2} \approx \sum_i k_i \sigma_i^2. \quad (2)$$

This margin formula is proved in the Appendix for the general model  $Y(\mathbf{X}) = \phi[U(\mathbf{X})]$ , where  $U$  is a quadratic function of the parameters  $\mathbf{X}$ . The actual yield surface response is more complicated, but we have seen in Sec. III that it is well approximated by a neural network. It is therefore interesting to know if this particular form of the yield satisfies the margin formula as well, that is if the inverse margin  $1/M$  could be obtained by a quadrature sum of the  $\sigma_i$ . We have checked this hypothesis with a metamodeling approach: A database of 1000 standard deviations  $\{\sigma_i, i=1, \dots, N\}$  was constructed in order to find the best values of the parameters  $k_i$ , and a validation base of 500 points was also created to estimate the RMSE. Both bases are LHSs and each standard deviation  $\sigma_i$  ranges from 1/4 to 4 times its nominal value given in Tables I and II. The robustness margin is computed for the nominal point that is with a DT gas density  $x_{20}=0.3 \text{ mg/cm}^3$  and  $x_{21}=x_{22}=0$ , as described in Sec. IV. Figure 11 shows the scatter plots for the predicted margin obtained with this model. The validation RMSE is 0.09: Eq. (2) gives an approximation of the margin with a precision of  $\pm 0.18$  at a confidence level of 95%. The RMSE decreases to 0.05 if we add the nondiagonal terms,

$$M^{-2} \approx \sum_{i,j} k_{ij} \sigma_i \sigma_j. \quad (3)$$

Figures 11 and 12 show that  $M^{-2}$  could be well approximated by a quadratic form of the standard deviations and that the

FIG. 12. Scatter plot for the prediction of the total margin with crossing terms  $i \neq j$ .

nondiagonal terms are not negligible: The surface  $Y=y_0$  is not exactly an ellipsoid or it is not well centered on  $\mathbf{X}=0$ . In any case, the margin formula, Eq. (1), is very useful in obtaining a first estimation of the overall margin and for comparing the effects of the different specifications. The main sources of errors are shown in Fig. 13: The total ablator thickness error is the dominant one and corresponds to a standard deviation of  $6 \mu\text{m}$  achieved at the beginning of this study. Since then, the CEA target fabrication laboratory has focused on this particular point and has achieved a tolerance of  $\pm 5 \mu\text{m}$  with a yield of 82% this year.<sup>19</sup> This has led to a standard deviation of about  $2 \mu\text{m}$ . The five following main contributors to the overall margin come from the experimental tuning errors. Although we have roughly estimated these uncertainties in this first study, it appears that their effects are very important and need to be precisely quantified in future work. Each item with a partial margin greater than 10 has a small impact on the robustness margin, but the overall contribution of these errors is not negligible as they are numer-

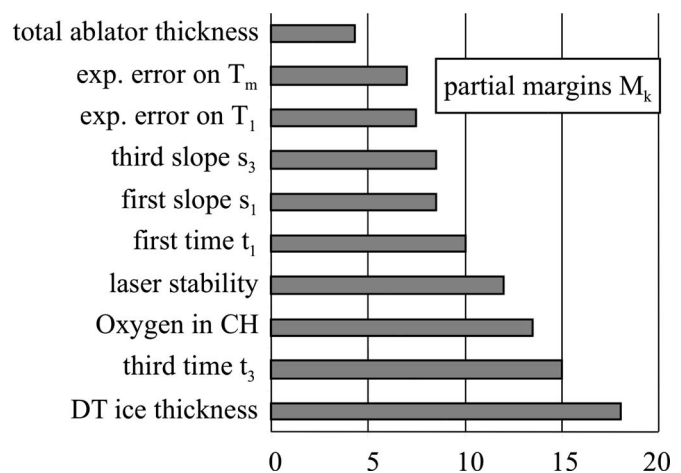


FIG. 13. Partial margins relative to the main sources of 1D-errors, whose specifications are given in Tables I and II.

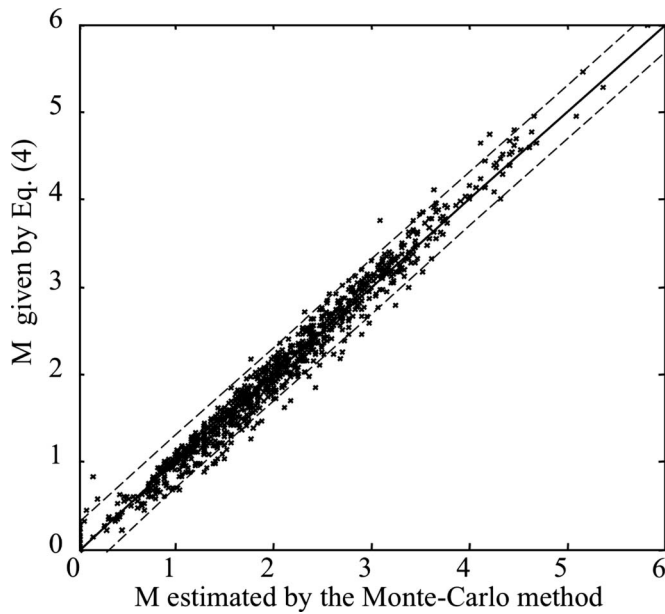


FIG. 14. Scatter plot for the prediction of the margin given by Eq. (4). The dashed lines are given at  $\pm 2$  RMSE.

ous: The net margin for these items is 4.8, which is of the same order as the ablator thickness margin (4.3) and the net rollup for the other items  $< 10$  (3.8).

As a general rule, the overall margin is a function of the vector of specified values  $\mathbf{x}$  and the PDFs of the independent random errors  $\mathbf{X}$ . In this paper we have assumed that these errors are Gaussian with zero mean so that  $M$  only depends on  $\mathbf{x}$  and the vector  $\sigma$  of all standard deviations. Let us denote by  $\mathbf{x}_0$  and  $\sigma_0$  the nominal point and specifications given in Tables I and II, which lead to the nominal margin  $M_0$ . We have studied the effects of  $x_{20}$  to  $x_{22}$  ( $\rho_{DT}$ ,  $\rho_{3He}$ , and DT preheating) for  $\sigma = \sigma_0$  in Sec. IV and the effects of  $\sigma$  for  $\mathbf{x} = \mathbf{x}_0$  above,

$$M(\mathbf{x}, \sigma_0) \approx F(u, x_{22})$$

for  $x_1$  to  $x_{19}$  and  $\sigma_0$  nominal; with  $u = \exp(x_{20} + 0.8x_{21})$  and  $F$  given by Eq. (1),

$$M(\mathbf{x}_0, \sigma)^{-2} \approx \sum_i k_i \sigma_i^2.$$

These two approximations raise a general margin model of the following form:

$$M(\mathbf{x}, \sigma) \approx M(\mathbf{x}_0, \sigma) F(u, x_{22}) / M_0 \text{ for } x_1 \text{ to } x_{19} \text{ nominal.} \quad (4)$$

We have checked the accuracy of Eq. (4) on a LHS data set of 1000 points where all standard deviations range from 1/4 to 4 times the nominal values and the two determinist parameters  $\rho_{3He}$  and DT preheating range from 0 to 0.2 mg/cm<sup>3</sup> and from 0 to 25  $10^{12}$  erg/g, respectively. The agreement is good as we can see in Fig. 14, with a RMSE of 0.15 between the two margin estimations.

## VI. CONCLUSIONS

The robustness of an ICF target must be assessed in a high-dimensional parameter space whose variables include fabrication defects and laser reproducibility. These input uncertainties induce a stochastic yield, in the sense that it will be different from shot to shot, and the possible robustness metrics are defined in terms of the yield probability density function. These metrics could be estimated from a great number of simulations where the inputs are sampled according to their PDF. In other words, a Monte Carlo method propagates the uncertainties through the numerical model. This could be computationally very expensive and, furthermore, the study has to be done again if the input standard deviations or the mean values are modified. The classical way to overcome this difficulty is to use a surrogate of the numerical code in the Monte Carlo estimation of the robustness metrics. Therefore a huge number of samplings can be run in order to obtain an accurate estimator. Haan and co-workers<sup>6,8</sup> proposed a surrogate based on a physical analysis of the minimum energy required for ignition: The 1D margin is determined as a function of velocity and entropy, which are obtained from the input variables  $\mathbf{X}$  with a low-order Taylor expansion. In this paper, we propose an alternative that consists of building an empirical surrogate from the database of simulations. The difficulty of this approach is to construct an accurate metamodel on a high-dimensional space with a very nonlinear response.

We tested this metamodeling approach on the 1D-robustness study of an indirect drive ICF capsule. The yield is well approximated by a neural network in a 22-dimensional space with a RMSE of 6% from a data set of about 2000 simulations. The metric we used is the margin  $M$  defined as the multiplier of all the specifications which induce a probability of 50% to exceed half the nominal yield. We estimated the margin sensitivity to the standard deviations of all random parameters, and toward the mean values of central gas densities and DT preheating. The two main results are the following:  $M^{-2}$  could be approximated by  $\sum_i M_i^{-2}$ , where  $M_i$  is the partial margin when  $X_i$  is the only random error; the margin depends on the partial gas densities via the sum  $\rho_{3He} + 0.8\rho_{DT}$ . This first robustness study has provided guidance for target fabrication research and development leading to improve the CEA's capabilities on the most sensitive parameters. A further conclusion of this study is the importance of the experimental tuning errors. These sources of errors were roughly estimated in this preliminary study and they need to be precisely quantified. Another promising application of the yield surrogate we have obtained is the possibility of optimization under uncertainties.<sup>20</sup> The neural network can be used to find the radiation temperature law that optimizes the margin, as the metamodel is accurate on the whole parameter space including all the pulse shape parameters.

In this paper, we demonstrate that a 1D-yield surrogate can be developed from a neural network and that the computational burden to develop training data can be greatly reduced by using an appropriate design of experiments to sample the parameter space. As neural networks are universal approximators,<sup>15</sup> they can also metamodel the fusion energy with 2D or 3D perturbations, as well as other outputs such as entropy or  $\rho R$  on direct or indirect drive. Therefore, we can apply the design of experiments strategy proposed by Issanchou and Gauchi,<sup>11</sup> which consists of running a first set

of simulations that is incrementally completed with the D-optimality criterion. This approach could be used to assess the capsule robustness as we did, and more generally to find relationships between input and output variables. This strategy will especially benefit to studies with expensive computing times.

#### APPENDIX: DEMONSTRATION OF THE MARGIN FORMULA FOR A QUADRATIC MODEL

From the analysis of the yield metamodel obtained in Sec. III, it appears that the levels sets of the output variable  $Y$  are approximate ellipses, centered on  $\mathbf{x}=0$ , whose axes are not necessary along the main axes. In particular, the relation  $Y(\mathbf{X}) > y_0$  defines a volume in the random input space that could be approximated by an ellipsoid. Therefore, the yield  $Y$  could be approximated by the following quadratic model:

$$Y(\mathbf{X}) = \phi[U(\mathbf{X})] \quad \text{with} \quad U(\mathbf{X}) = \sum_{i,j=1}^N a_{ij} X_i X_j,$$

where  $\phi$  is a continuous, decreasing function from  $[0, \infty)$  into  $[0, Y_{\max}]$  with  $\phi(u_0) = y_0$ , and  $\mathbf{a}$  is a positive-definite matrix.

Let us define the partial margin  $M_i$  as the highest multiple of the nominal requirement that returns at least a yield  $y_0$ , in simulations in which  $X_i$  is the only error,

$$Y(0, \dots, X_{0i}^{\pm}, \dots, 0) = y_0$$

with

$$X_{0i}^{\pm} = \pm M_i^{\pm} \sigma_i, \quad M_i = \min(M_i^+, M_i^-).$$

The partial margins  $M_i$  are then simply given by  $u_0 = a_{ii} M_i^2 \sigma_i^2$  and the total margin  $M$  verifies  $P_M(U < u_0) = P_0$ . Our purpose is to prove that the margin formula, Eq. (2), is valid for this model. The first main hypothesis is that the input random vector  $\mathbf{X}$  consists of independent random variables. If this is not the case, one should first map the input random vector into a set of independent random variables. For instance, the Rosenblatt transform maps a continuous random vector with known marginal and conditional distribution functions into a random vector of independent Gaussian random variables.<sup>16</sup> In this 1D-robustness study, the number of independent random variables is  $N=23$ . The following results use the fact that the number of random variables  $N$  is large and that non particular input  $X_i$  is dominant. They are robust with respect to the PDFs of the random variables, as long as they have finite variances. By the central limit theorem, the random variable  $U(X)$  has a Gaussian distribution with mean value  $\langle U \rangle$  and variance  $s^2$ ,

$$U \approx \langle U \rangle + sZ,$$

where  $Z$  is the normal distribution  $N(0, 1)$ ;

$$\langle U \rangle = \sum_{i=1}^N a_{ii} \sigma_i^2,$$

$$s^2 = \sum_{i=1}^N a_{ii}^2 (\langle X_i^4 \rangle - 3\sigma_i^4) + \sum_{i,j=1}^N (a_{ij}^2 + a_{ij} a_{ji}) \sigma_i^2 \sigma_j^2.$$

The probability distribution  $P_M$  is then estimated by

$$P_M(U < u_0) \approx P_M(\langle U \rangle + sZ < u_0) = P\left(sZ < \frac{u_0}{M^2} - \langle U \rangle\right).$$

Using the symmetry of the normal distribution  $N(0, 1)$ , we find that this probability is equal to 1/2 when  $u_0/M^2 = \langle U \rangle$ , which gives

$$M^{-2} \approx \sum_i \frac{a_{ii} \sigma_i^2}{u_0} = \sum_i M_i^{-2}.$$

The margin formula holds true as soon as the yield contour  $Y=y_0$  is an ellipsoid centered on  $\mathbf{X}=0$  and the probability level  $P_0$  equals 1/2. It takes a form independent of the non-diagonal terms  $a_{i \neq j}$  of the matrix  $\mathbf{a}$ . If we were looking for another probability level,  $s^2$  would play a critical role and the result would be more complicated.

<sup>1</sup>D. Besnard, *Eur. Phys. J. D* **44**, 207 (2007).

<sup>2</sup>J. D. Lindl, *Inertial Confinement Fusion, the Quest for Ignition and Energy Gain Using Indirect Drive* (Springer-Verlag, New York, 1998).

<sup>3</sup>P. A. Holstein, J. Bastian, C. Bowen, M. Casanova, F. Chaland, C. Cherfils, E. Dattolo, D. Galmiche, P. Gauthier, J. Giorla, S. Laffite, S. Liberatore, P. Loiseau, O. Larroche, L. Lours, G. Malinié, L. Masse, M. C. Monteil, O. Morice, D. Paillard, F. Poggi, Y. Saillard, P. Seytor, D. Teychenné, M. Vandenboomgaerde, F. Wagon, M. Bonnefille, T. Hedde, E. Lefebvre, G. Riazuelo, D. Babonneau, M. Primout, A. Casner, S. Depierreux, F. Girard, G. Huser, J. P. Jadaud, D. Juraszek, J. L. Miquel, M. Naudy, F. Philippe, C. Rousseaux, and L. Videau, "Review of studies for thermonuclear ignition with 1.8 MJ laser (LMJ): Theory and experiment," CEA Report No. R-6182, 2008.

<sup>4</sup>S. W. Haan, M. C. Herrmann, J. D. Salmonson, P. A. Amendt, D. A. Callahan, T. R. Dittrich, M. J. Edwards, O. S. Jones, M. M. Marinak, D. H. Munro, S. M. Pollaine, B. K. Spears, and L. J. Suter, *Eur. Phys. J. D* **44**, 249 (2007).

<sup>5</sup>J. Giorla, F. Poggi, D. Galmiche, P. Seytor, R. Quach, C. Cherfils, P. Gauthier, S. Laffite, and L. Masse, *Fusion Sci. Technol.* **51**, 514 (2007).

<sup>6</sup>S. W. Haan, J. Salmonson, D. Clark, D. Callahan, B. Hammel, L. Suter, J. Edwards, and J. Lindl, *Bull. Am. Phys. Soc.* **52**, 40 (2007).

<sup>7</sup>J. Salmonson, *Bull. Am. Phys. Soc.* **52**, 273 (2007).

<sup>8</sup>D. S. Clark, S. W. Haan, and J. D. Salmonson, *Phys. Plasmas* **15**, 056305 (2008).

<sup>9</sup>O. S. Jones, J. L. Milovich, D. A. Callahan, S. W. Haan, and C. C. Widmayer, *Bull. Am. Phys. Soc.* **52**, 357 (2007).

<sup>10</sup>K.-T. Fang, R. Li, and A. Sudjianto, *Design and Modeling for Computer Experiments* (Chapman and Hall/CRC, New York, 2006).

<sup>11</sup>S. Issanchou and J.-P. Gauchi, *Neural Networks* **21**, 945 (2008).

<sup>12</sup>M. Vandenboomgaerde, J. Bastian, A. Casner, D. Galmiche, J.-P. Jadaud, S. Laffite, S. Liberatore, G. Malinie, and F. Philippe, *Phys. Rev. Lett.* **99**, 065004 (2007).

<sup>13</sup>C. Cherfils-Clérouin, M. Bonnefille, E. Dattolo, F. Fremerye, D. Galmiche, P. Gauthier, J. Giorla, S. Laffite, S. Liberatore, P. Loiseau, G. Malinie, L. Masse, F. Poggi, and P. Seytor, *J. Phys.: Conf. Ser.* **112**, 022023 (2008).

<sup>14</sup>P. Seytor, D. Galmiche, and C. Cherfils, *J. Phys. IV* **133**, 187 (2006).

<sup>15</sup>G. Dreyfus, *Neural Networks, Methodology and Applications* (Springer-Verlag, Berlin, 2005).

<sup>16</sup>M. Rosenblatt, *Ann. Math. Stat.* **23**, 470 (1952).

<sup>17</sup>K. Q. Ye, *J. Am. Stat. Assoc.* **93**, 1430 (1998).

<sup>18</sup>V. V. Fedorov, *Theory of Optimal Experiments* (Academic, New-York, 1972).

<sup>19</sup>G. Legay, M. Theobald, J. Barnouin, E. Pêche, S. Bednarczyk, C. Hermereel and O. Legaie, "Thickness, doping accuracy and roughness control in graded germanium doped CHx microshells for LMJ," *Fusion Sci. Technol.* (to be published).

<sup>20</sup>A. A. Giunta, M. S. Eldred, T. G. Trucano, and S. F. Wojtkiewicz, Jr., paper AIAA-2002-1642 in 43rd AIAA/ASME/ASCE/AHS/ASC Structures, Structural Dynamics, and Materials Conference (Nondeterministic Approaches Forum), Denver, CO, 22–25 April 2002(b), p. 1642.